Heteroepitaxial growth of the intrinsic vacancy semiconductor Al_2Se_3 on Si(111): Initial structure and morphology

Chih-Yuan Lu,[1,2,*] Jonathan A. Adams,[3,†] Qiuming Yu,[2] Taisuke Ohta,[1,2,‡] Marjorie A. Olmstead,[3,2] and Fumio S. Ohuchi[1,2,§]
[1]*Department of Materials Science and Engineering, University of Washington, Seattle, Washington 98195-2120, USA*
[2]*University of Washington Center for Nanotechnology, Seattle, Washington 98195-2140, USA*
[3]*Department of Physics, University of Washington, Seattle, Washington 98195-1560, USA*
(Received 9 January 2008; published 25 August 2008)

The evolution of nanostructure morphology and local chemical environment during heteroepitaxial growth of aluminum selenide on Si(111) was investigated with scanning tunneling microscopy and high-resolution photoemission spectroscopy. Despite the strong similarity to GaSe in atomic and electronic structure during deposition of the first AlSe bilayer, subsequent growth is quite different—resulting in an alternating Al-Se-Al-Se stacking sequence consistent with defected-wurtzite-structure Al_2Se_3. The first bilayer is completed on a given terrace before the second layer nucleates, but subsequent layers nucleate before completion of the second layer. The surfaces of well-formed Al_xSe_y islands are smooth and terminated by Se atoms; Al then sticks before additional Se, resulting in rougher incomplete islands with Al-rich disordered surfaces. Growth with extra Al in the incident flux does not result in layered AlSe and induces only subtle differences in film morphology.

DOI: 10.1103/PhysRevB.78.075321 PACS number(s): 68.55.ag, 68.35.bg, 68.37.Ef, 79.60.Jv

I. INTRODUCTION

Semiconductors based on compounds consisting of group III and group VI elements are of interest both for the physics associated with their intrinsic vacancy structures and for their significant promise as future device materials. These chalcogenide semiconductors have band gaps and lattice constants similar to those of many more common electronic materials but their thin-film growth is much less studied.[1–11] M_2X_3 compounds (where M=Al, Ga, or In and X=S, Se, or Te) exhibit structures based on the zinc-blende or wurtzite structure of tetrahedrally bonded III-V and II-VI semiconductors, but with one-third of the cation sites are vacant. Intrinsic vacancies in the most common structures of bulk Al_2Se_3, Ga_2Se_3, and In_2Se_3 are localized along helices[12] (also found for γ-In_2Se_3),[13,14] lines,[15,16] and planes,[17] respectively. This makes M_2X_3 materials intriguing candidates for functionalization through vacancy ordering (e.g., by creating anisotropic optical properties)[13,18,19] and/or occupation of the vacancies by additional elements (e.g., transition metals).[20] The lattice constants of both Ga_2Se_3 and Al_2Se_3 are close to that of Si (0.1% and 1.3% mismatch, respectively), leading to the possibility of combining the unique properties of these intrinsic vacancy materials with silicon technology. Successful application of these materials to silicon technology, however, requires understanding their heteroepitaxy on silicon substrates. The atomic and electronic structure of the first layer of Al_xSe_y on Si(111) (Ref. 7) is very similar to that of Ga_xSe_y.[3,4,6,9] Both form a single M-Se bilayer (BL) (M=Al,Ga) with Si-M bonding normal to the surface and an M-Se bond in a direction that continues the diamond (zinc-blende) structure of the substrate (Se in a hollow site). The Si-M and M-Se bond lengths and angles are within 0.02 Å and 2°, respectively, on the two surfaces;[3,4,7] the surface Se exhibits a fully occupied lone-pair state of similar energy and dispersion on both.[6,7] Despite this similarity in atomic and electronic structure, the AlSe-terminated surface is far more reactive than GaSe-terminated Si(111). While GaSe/Si(111) does not react under atmospheric exposure, AlSe/Si(111) reacts strongly with O_2, H_2O, and the atmosphere.[8]

Aluminum and gallium selenides exhibit different bulk structures. Al_2Se_3 and Ga_2Se_3 form defected wurtzite[12] and zinc-blende[15,16] structures, respectively. Gallium and selenium also exhibit a layered structure GaSe with van der Waals bonding between covalently bonded Se-Ga-Ga-Se layers; InSe takes a similar structure. An equivalent layered structure AlSe, however, has not been reported. The interface BLs of both AlSe and GaSe on Si have very similar atomic and electronic structure to bulk layered GaSe (Ref. 6) and subsequent growth of Ga_xSe_y on Si(111):GaSe results in layered GaSe.[1] This raises the possibility that layered AlSe may be stabilized through epitaxy on AlSe-terminated Si (Si-Al-Se::Se-Al-Al-Se) as found for GaSe.

This paper reports a detailed study of the initial stages of Al_xSe_y heteroepitaxy on Si(111) using *in situ* scanning tunneling microscopy (STM) and high-resolution core-level photoemission spectroscopy (PES). We find that Al_xSe_y grows in an Al-Se-Al-Se sequence, consistent with bulk Al_2Se_3 and not a layered AlSe compound, even when an Al_2Se_3 source is supplemented with extra Al. STM reveals the interface AlSe BL to be less ordered than GaSe/Si(111),[9] which likely contributes to its increased reactivity. Both STM and PES show a bulklike Al_2Se_3 structure within the first two layers, including two distinct Se environments and development of bulklike photoelectron-diffraction patterns. Thicker films displayed a $(\sqrt{3}\times\sqrt{3})R30°$ low-energy electron-diffraction (LEED) pattern consistent with the known bulk $\sqrt{3}$ vacancy ordering in (0001) planes.

II. EXPERIMENTAL DETAILS

Aluminum selenide was evaporated from Al_2Se_3 granules heated in a graphite crucible to temperatures between 950 and 960 °C, yielding a flux of a few angstroms per minute as measured by a quartz-crystal monitor. The silicon substrate temperature was held constant in the range of 550–625 °C

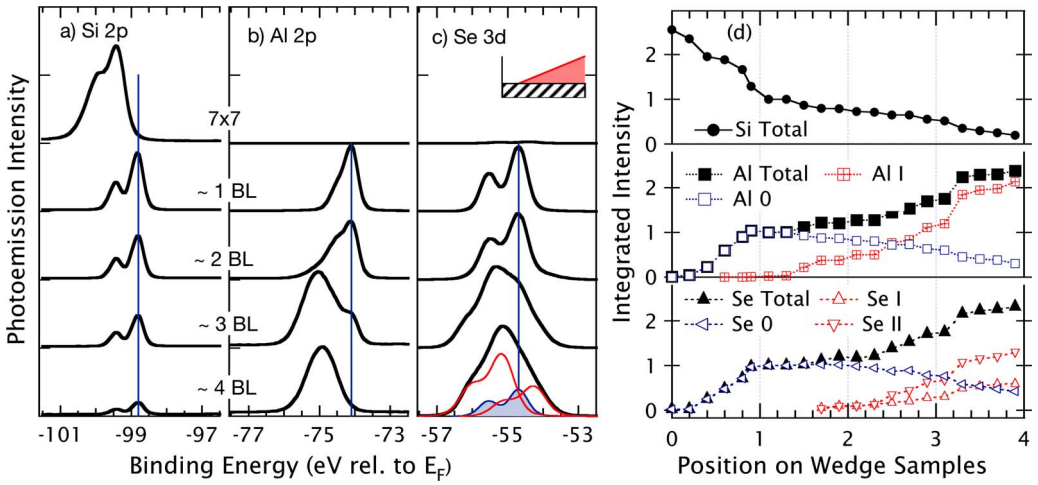

FIG. 1. (Color online) Photoemission of Al_2Se_3 deposition on Si(111). (a)–(c) Spectra from wedge film 0 to 4 BL thick (see inset). Al_2Se_3 flux=6.5 Å/min; T_{sub}=550 °C. Photon energy $h\nu$=185 eV. (a) Si 2*p*, (b) Al 2*p*, and (c) Se 3*d*. Vertical (blue) lines mark peak ($2p_{3/2}$ or $3d_{5/2}$) for single BL. Fitted Se 3*d* components are shown for the thickest film. (d) Intensity of fitted components vs position. Component energy was held constant during fitting. Points between 0 and 1 are from a 0–1 BL wedge (Al_2Se_3 flux=1.6 Å/min, 625 °C, and $h\nu$ =240 eV); points between 1 and 4 are from the same 0–4 BL wedge as (a)–(c). Position 1 corresponds to a single BL for each sample; spectra from both samples are normalized to 1 at this position. Varying sticking coefficients with coverage results in a monotonic, but not necessarily linear, dependence of thickness on position.

during deposition. Some experiments also utilized additional Al (Al_2Se_3:Al flux ratio of 1:1) to test whether growth of layered AlSe could be induced by increasing the Al chemical potential. Samples were transferred under ultrahigh vacuum for STM[21] or PES measurements.

Photoemission measurements were performed on graded thickness (wedge-shaped) epitaxial layers of Al_2Se_3 on Si(111) substrates to allow comparison of different thickness films under identical growth and measurement conditions. Wedge samples were grown by moving a shutter across the sample during deposition. The nominal thickness variation over the 50-micron-spot size of the synchrotron beam is less than 0.03 BL. One BL consists of two Si monolayers (MLs) or one Al-Se layer of thickness equal to the minimum (0001) or (111) step height (bulk Al_2Se_3 BL=3.17 Å and bulk Si BL=3.13 Å).

III. RESULTS

Below, we first discuss core-level photoemission results showing the evolution of the stoichiometry and local chemical environments with thickness, followed by detailed STM measurements of both the initial interface bilayer formation and subsequent overlayer growth, with and without extra Al in the incident flux. We also show the development of the band structure with thickness.

A. Core-level PES

High-resolution core-level spectra as a function of film thickness are shown in Fig. 1 for both the Si substrate [Fig. 1(a)] and Al_xSe_y overlayer (Al 2*p* [Fig. 1(b)] and Se 3*d* [Fig. 1(c)]). The inset schematically shows the wedge sample (0–4 BL). The relative intensities of the fitted components (see below) are shown as a function of position on two wedge samples (0–1 and 0–4 BL) in Fig. 1(d). Due to the strong coverage dependence of the sticking coefficient (much higher for the first layer than the second, then increased again for the third), conversion from position to coverage is only approximate. Lower flux and higher substrate temperatures were used for the thinner sample (see caption).

The unexposed Si shows Si 2*p* emission characteristic of clean Si(111)7×7 and no Al or Se emission (Fig. 1). As Al and Se begin to stick, the Si 2*p* attenuates and changes shape until, at about 1-BL thickness, a single spin-orbit-split component is observed. The narrow Si 2*p* peak is shifted 0.6 eV to lower-binding energy (LBE) relative to the main 7×7 emission, indicating a new Fermi-level position close to the valence-band maximum. The single-component Si, Al, and Se spectra at this thickness are equivalent to those previously reported for AlSe-terminated Si(111) (Ref. 7), and the relative intensity of the Se 3*d* and Si 2*p* peaks measured with Mg K_α x-ray photoelectron spectroscopy (XPS) is within our estimated error of that for the well-characterized GaSe bilayer on Si(111).[3,4] With deposition beyond 1 BL, the Si 2*p* exhibits no significant change other than attenuation as the overlayer film becomes thicker [Figs. 1(a) and 1(d)], while the Al and Se emission each show additional components growing while the interface emission [peaks at position of vertical (blue) lines] is attenuated. A new broad Al 2*p* component appears, which is shifted ~0.9 eV to higher-binding energy (HBE) from the original peak. The intensity of this HBE peak [labeled Al I in Fig. 1(d)] steadily increases with thickness while the original peak (labeled Al 0) attenuates, appearing only as a shoulder at 3–4 BL. The Se 3*d* emission [Fig. 1(c)] exhibits two additional components with increasing thickness but not until the Al I component is well established; the initial Se 0 component is attenuated as the new components grow. One overlayer Se component (labeled Se I) is shifted 0.57 eV to HBE from the original Se 0 compo-

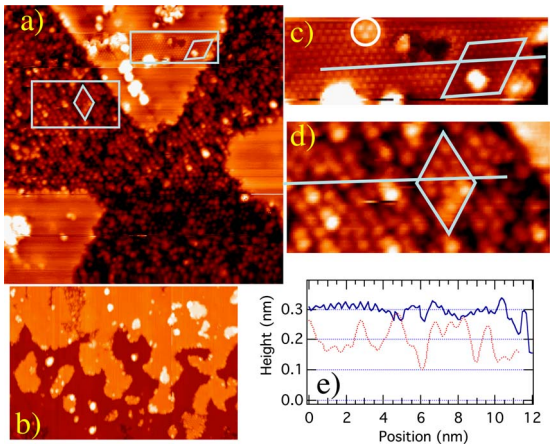

FIG. 2. (Color online) Bilayer formation. STM images of $\lesssim$1 ML Al plus Se deposited from combined Al_2Se_3 and Al sources at T_{sub}=550 °C. (a) 39×39 nm^2 (−2.6 V, 0.12 nA, empty state). (b) 88×44 nm^2 (−2.32 V, 0.17 nA) in higher coverage region. (c) 14×4.6 nm^2, enlargement of upper rectangle in (a), showing atomic resolution of AlSe BL; circle highlights a defect similar to the most common defect on GaSe/Si(111). (d) 14×7 nm^2, enlargement of lower rectangle in (a). (e) Tip height vs position along lines parallel to $\langle 1\bar{1}0\rangle$ drawn on images (c) (solid blue line) and (d) (dotted red line). Rhombuses in (a), (c), and (d) denote 7×7 substrate unit cell for reference.

nent and the other (Se II) is shifted 0.48 eV to LBE. The three fitted components are shown for the ~4 BL spectrum in Fig. 1(c) (Se 0 is shaded) with their relative intensities as a function of thickness shown in Fig. 1(d). Comparison of the intensities of the Si, Al, and Se components as a function of position reveals that in the first layer, Al and Se accumulate at roughly the same rate, while in the second layer, Al sticks to the surface before Se. The two "bulk" Se components (Se I and Se II) begin to appear after the second Al layer nucleates and increase steadily in a 2:1 ratio with increasing film thickness. The interface Al and Se components (Al 0 and Se 0) are attenuated as the overlayer thickness increases.

XPS measurements on thicker films (Al_2Se_3 source, 8 nm thick) show two Se 3*d* components separated by 1.06±0.02 eV with a ratio of 2.15:1 in normal emission and photoelectron-diffraction signatures consistent with wurtzite; the energy difference $\Delta_{Al\text{-}Se}$ between the Al $2p_{3/2}$ and Se I $3d_{5/2}$ is 19.76±0.04.[22] The two bulklike Se components in Fig. 1(c) are separated by 1.05±0.02 eV and $\Delta_{Al\text{-}Se}$ =19.79±0.04 eV for the equivalent bulklike components.

B. STM of bilayer formation

The growth morphology of heteroepitaxial Al_xSe_y on Si was investigated with STM. Given the AlSe stoichiometry found with PES for the first BL, despite an Al_2Se_3 source, we supplemented the Al_2Se_3 source with extra Al for the data presented in Fig. 2. The extra Al resulted in slightly better ordering of the surface (see below), but no other significant differences for the first BL. Figure 2 shows STM images from a 39×39 nm^2 region of a film deposited with both Al_2Se_3 and Al sources at substrate temperature T_{sub} =550 °C. Area averaged XPS showed the Al coverage to be just under 1 ML and the Se coverage slightly less; the particular region shown in Figs. 2(a), 2(c), and 2(d) has sub-ML average coverage, while Fig. 2(b) shows a larger (88×44 nm^2) region on a similarly prepared sample with a nearly complete BL. The surface shows two types of regions: "rough" (0.1–0.2 nm corrugation) and "smooth" (~0.01 nm corrugation). The borders of the triangular smooth regions are generally parallel to $\langle 1\bar{1}0\rangle$. A smooth region (upper rectangle) is enlarged in Fig. 2(c); it shows hexagonally symmetric atomic corrugations similar to those of GaSe-terminated Si(111),[9] where the high points were attributed Se lone-pair orbitals. Atomic resolution on this AlSe-terminated surface is much more difficult to obtain and sustain than on GaSe/Si(111). The circle highlights a defect consisting of three bright dots on an equilateral triangle. This defect strongly resembles the most common point defect observed on GaSe/Si(111), labeled D1 in Ref. 9, which is attributed to a point atomic substitution and appears only on domains where the Ga-Se bond is parallel to a Si-Si bond (zinc-blende continuation of the Si lattice). The dark triangle below and to the right of the circled defect resembles a D4-type defect observed[9] on GaSe/Si(111). The upper linescan in Fig. 2(e) (blue solid line) shows the ~0.01 nm corrugation with 0.38 nm periodicity of the smooth BL (seven spots across the 7×7 rhombus along $\langle 1\bar{1}0\rangle$) plus the larger scale defects. On a larger scale, Fig. 2(b) shows a region of nearly complete smooth BL coverage. The local step structure is highly convoluted, with numerous small islands, unlike the smooth parallel steps observed for the starting 7×7 surface. The overall step structure, however, is preserved at larger scales [see 180×180 nm^2 images in Figs. 3(a) and 3(d)]. An area of the rough region in Fig. 2(a) (lower rectangle) is enlarged in Fig. 2(d) with a topographic linescan along $\langle 1\bar{1}0\rangle$ shown as the lower linescan in Fig. 2(e) (red dotted line). The rough region contains arrays of high spots with approximately the same 2×2 spacing and orientation as the adatoms on the starting Si(111)7×7 reconstruction. Some areas still show the deep corner holes of the starting reconstruction [highlighted by 7×7 rhombus in Fig. 2(d)], but the high spots generally align in longer rows along $\langle 1\bar{1}0\rangle$ with frequent "missing spots." The observed reconstruction is different from that reported for pure Al on Si(111),[23] which results in $\sqrt{3}$ or $\sqrt{7}$ periodicity, indicating that both Al and Se are likely involved in disrupting the 7×7 reconstruction as the AlSe BL forms. The apparent height difference between the corner holes and the smooth region is about 3/4 the 0.32-nm-BL step height of Si or Al_2Se_3, while most of the bright dots have an intermediate height about 0.06 nm below the smooth region. It should be noted that it is unlikely the STM tip measures the true depth of these subnanometer diameter "holes."

C. Nucleation of Al_2Se_3 overlayer

The photoemission results (Sec. III A) show completion of the first AlSe BL before nucleation of additional local

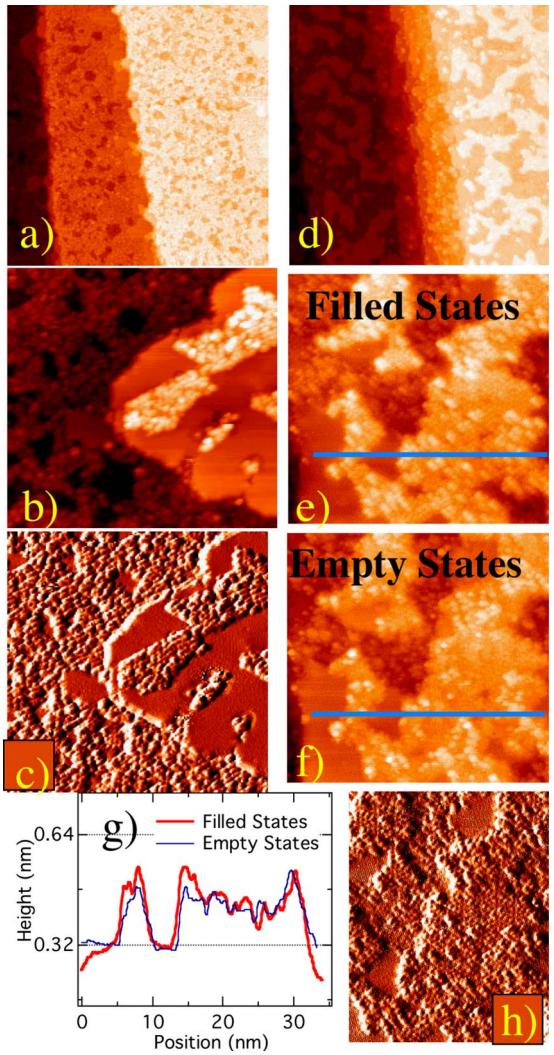

FIG. 3. (Color online) Overlayer nucleation and growth of Al_2Se_3. (a)–(c) ~1.6 BL Al_xSe_y deposited at T_{sub}=585 °C with both Al_2Se_3 and Al sources. (a) 180×180 nm^2, z scale of 2.65 nm. (b) 39×39 nm^2 (–2.7 V, 0.19 nA). (c) Horizontal gradient of (b). (d)–(h) ~1.8 BL, single source. (d) 180×180 nm^2, z scale of 2.65 nm. (e) 37×37 nm^2 occupied state image (–2.4 V, 0.16 nA). (f) Same region (and color scale) as (e); empty-state image (+2.4 V, 0.16 nA). (g) Height profiles along lines in (e) and (f). (h) Horizontal gradient of (f).

environments; similar results are found with STM. Figure 3 shows STM of about 1.6–1.8 BL of Al_2Se_3 deposited at T_{sub}=585 °C. Both Al_2Se_3 and Al sources were used for Figs. 3(a)–3(c); only an Al_2Se_3 source was used for the film in Figs. 3(d)–3(h). Above 1 BL, the surface again shows rough and smooth regions, although the smooth regions in Fig. 2(b) are now the lower heights on each terrace in Fig. 3, while the rough regions appear as islands on the smooth background. No evidence of the initial 7×7 structure remains. The lowest areas are similar to the smooth regions in Fig. 2 and are presumed to be a complete interface BL. The highest points on the rough regions are near the height expected for a complete BL, exhibiting 0.1–0.2 nm corrugation on a 1–2-nm-length scale. The 2-BL-high island at the right of the image in Fig. 3(a) is locally the same as the region

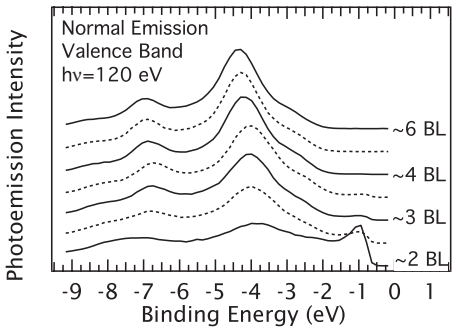

FIG. 4. Development of valence-band structure with thickness. Normal emission at photon energy $h\nu$=120 eV. Wedge sample, ~2–6 BL, T_{sub}=550 °C, single source Al_2Se_3, flux=6.5 Å/min.

surrounding it, as evidenced by the gradient image. The island is thus likely a 2-BL-high Si island terminated with an AlSe bilayer and subsequent overlayer nucleation. Small regions of height 1 BL above the surrounding terrace may also be seen at the edge of the main island.

The effect of the stoichiometry of the incident flux may be seen by comparing Figs. 3(a)–3(c) with Figs. 3(d)–3(h), which are of comparable total thickness (~1.7 BL) with [Figs. 3(a)–3(c)] and without [Figs. 3(d)–3(h)] extra Al. Both show a smooth completed BL as the lowest exposed layer and both rough and smooth regions. Comparison of Fig. 3(a) and Fig. 3(d) shows that the large-scale morphology is similar for the two cases; the size and shape of the islands differs somewhat, but we cannot rule out different local coverage or step structure as a cause. The small-scale (37 nm) image from the pure Al_2Se_3 deposition sample [Figs. 3(e) and 3(f)] has smaller smooth islands and more dispersed nucleation and growth of the next BL than that with extra Al [Fig. 3(b)]. The local structure of the rough and smooth regions, however, is quite similar under the two deposition conditions [see gradient images Figs. 3(c) and 3(h)]. The BL is covered first by a layer about half the height of a full BL. The gradient image in Fig. 3(h) shows a local pattern consistent with a $(\sqrt{3}\times\sqrt{3})R30°$ reconstruction; its height is independent of bias voltage but close to the noise level. The highest regions appear to nucleate only when that layer is nearing completion and look taller in occupied state images than in empty-state images.

D. Valence band

The development of the valence-band structure with film thickness is shown in Fig. 4. The peak just below the Fermi level at low coverage is associated with the Se lone-pair emission from the interface AlSe BL.[7] In spectra of the pure BL at both $h\nu$=130 and 21.2 eV, this peak dominates the spectrum.[7,22] This interface peak is no longer visible at a thickness above ~3 BL, while bulklike features, including a shoulder about 2.5 eV binding energy, are established at 2–3 BL and remain unchanged with further coverage except for a gradual Fermi-level shift.

IV. DISCUSSION

The structure of the complete AlSe interface BL on Si(111) has been previously shown with photoelectron

diffraction[7] to be very similar to that of GaSe/Si(111),[3,4] although it is much more reactive.[8] We have also found that the range of temperature and flux for which the growth self-limits at a single BL is much narrower for Al_xSe_y growth than for GaSe deposition.[22] We did not observe clear self-limiting behavior when the Al_2Se_3 flux was supplemented with Al, but it may self-limit at lower fluxes and/or higher substrate temperatures than were investigated. Figure 2(b) shows the local structure of the completed AlSe/Si(111) BL (including the point defects) to be similar to GaSe/Si(111), but the uniformity and stability are inferior on the AlSe-terminated surface. The large number of defects and rough island edges on the surface likely accounts for the increased reactivity of AlSe/Si(111) over GaSe/Si(111). The increased affinity for adsorbates likely also contributes to the difficulty in obtaining high-resolution images of the AlSe BL structure.

The PES measurements, where films were deposited with a single Al_2Se_3 source, show Al and Se sticking more or less simultaneously for the first BL. In the case of dual source deposition ($Al+Al_2Se_3$), STM shows disruption of the local Si(111)7×7 structure (possibly with exchange of Si adatoms for Al and/or Se) coexisting with regions of complete AlSe BL termination. Adatoms on the Si(111) surface bond to three Si dangling bonds, so that trivalent Al has a larger contribution to empty state than to filled-state images while tetravalent Si is similar in each, leading to a possible association of the brightest spots in the empty-state image of Fig. 2(d) with Al adatoms at sub-ML coverage. This is contrary to the typical interaction of pure Al with Si(111),[23] but the presence of Se and the need to remove the Si adatoms to create the AlSe BL may lead to a different interaction. The local island and step structure in Fig. 2(b) is indicative of significant overall movement of Si and is similar to that seen on GaSe/Si(111).[9]

After completion of the first BL, the second layer begins to nucleate (Fig. 3). The initial structure appears similar in height in both filled and empty-state images, while the regions where the layer is highest are taller in filled state images. This is consistent with the PES results indicating that a significant fraction of an Al layer sticks to the completed BL before second-layer Se begins to stick, even with a single source, since Al bonding to the passivated AlSe-terminated Si(111) layer would be expected to exhibit both full and empty states, while Se bonding to this structure should have more occupied states. The step heights observed in STM are those of a single BL (0.32 nm) and not the quadlayer ($\sim$0.8 nm) associated with layered III-VI materials. While Al sticks before Se, it appears to self-limit to a film that is locally 1 ML or less. Once the Al layer is completed locally (perhaps at 2/3 coverage as in the bulk crystal), the Se can stick and complete the BL. This initial sticking of Al, combined with the absence of a layered bulk AlSe phase (from which we infer that AlSe has a higher energy than Al_2Se_3), preclude nucleation of layered AlSe even though the first BL has a lone-pair termination similar to layered GaSe.

Photoemission shows the second layer already displays distinct bulklike chemical environments—one bulk environment for Al atoms and two for Se. The energy spacings are the same for the 2–4 layer film and one ten times that thickness. The bulk valence-band structure starts with the second BL and is established by the third one (Fig. 4); these same environments persist to very thick films. In bulk Al_2Se_3 there are two distinct Se sites: 2/3 of the Se atoms have three Al atoms and one Al vacancy as nearest neighbors, while the remaining 1/3 of the Se atoms are adjacent to two Al atoms and two vacancies. Similar chemical environments have been observed in growth of defected zinc-blende $Ga_2Se_3/Si(100)$, where Ga has one chemical site and Se has two chemical sites arising from the same nearest-neighbor environment as for the wurtzite structure; the separation between the two Se $3d$ components is again just over 1 eV.[10] Angle-resolved valence-band spectra taken with $h\nu=21.2$ eV on an 8 nm Al_2Se_3 film[22] showed weakly dispersing states at $\sim$2.5 and $\sim$4 eV below the Fermi level similar to the $\vec{k}=0$ states in Fig. 4. These results show that the local structural and electronic environment of $Al_2Se_3/Si(111)$ is established in the first 2–3 BL. In bulk Al_2Se_3, the intrinsic vacancies form a $(\sqrt{3}\times\sqrt{3})R30°$ pattern in the (0001) plane [equivalent to the (111) plane of zinc blende]. We observed a $(\sqrt{3}\times\sqrt{3})R30°$ LEED pattern on thick (8 nm) films, but observed neither any obvious vacancy-induced reconstruction with STM nor LEED superstructure on thin ($\lesssim$2 nm) films. There is a hint of $(\sqrt{3}\times\sqrt{3})R30°$ pattern in the gradient image of Fig. 3(h), but it was not seen in any other images. It thus appears that the vacancy ordering requires at least a few unit cells to become well established.

V. SUMMARY

Despite the strong similarity between the interface BLs of GaSe/Si(111) and AlSe(111), as previously established with photoemission and confirmed here with atomic resolution STM, growth of subsequent layers is quite different. The combination of STM, core-level photoemission, and valence-band photoemission data shows that a local Al_xSe_y structure similar to the bulk defected-wurtzite structure is established, in contrast to the layered GaSe obtained under similar conditions for GaSe/Si(111). After completion of the first BL, the film grows by Al sticking first and then Se completing the layer locally. Even when extra Al is added to the incident flux, a layered AlSe film is not produced. Rather, the overlayer structure continues to take the III-VI stacking sequence (Al-Se-Al-Se). Supplying extra Al makes minimal changes in the local morphology.

ACKNOWLEDGMENTS

This work was supported by NSF Grants No. DMR-0102427 and No. 0605601 and by the M. J. Murdock Charitable Trust. T.O. further acknowledges the support from the UW-CNT University Initiative Fund. Some data were obtained at the Advanced Light Source in Berkeley, CA (DOE Contract No. DE-AC03-76SF00098). J.A.A. and C.Y.L. submitted portions of this work in partial fulfillment of the requirements for the Ph.D. at the University of Washington.

*Present address: Intel Corporation, 5200 NE Elam Young Parkway, Hillsboro, OR 97124.
†Present address: Advanced Portfolios Ltd., London, UK.
‡Present address: Sandia National Laboratories, Albuquerque, NM.
§ohuchi@u.washington.edu

[1] Le Thanh Vinh, M. Eddrief, John E. Mahan, André Vantomme, J. H. Song, and Marc-A. Nicolet, J. Appl. Phys. **81**, 7289 (1997).
[2] A. Koebel, Y. Zheng, J. F. Pétroff, J. C. Boulliard, B. Capelle, and M. Eddrief, Phys. Rev. B **56**, 12296 (1997).
[3] S. Meng, B. R. Schroeder, and M. A. Olmstead, Phys. Rev. B **61**, 7215 (2000).
[4] S. Meng, B. R. Schroeder, A. Bostwick, M. A. Olmstead, E. Rotenberg, and F. S. Ohuchi, Phys. Rev. B **64**, 235314 (2001).
[5] R. Rudolph, C. Pettenkofer, A. Klein, and W. Jaegermann, Appl. Surf. Sci. **167**, 122 (2000).
[6] R. Rudolph, C. Pettenkofer, A. A. Bostwick, J. A. Adams, F. S. Ohuchi, M. A. Olmstead, B. Jaeckel, A. Klein, and W. Jaegermann, New J. Phys. **7**, 108 (2005).
[7] J. A. Adams, A. Bostwick, T. Ohta, Fumio S. Ohuchi, and Marjorie A. Olmstead, Phys. Rev. B **71**, 195308 (2005).
[8] J. A. Adams, A. Bostwick, Fumio S. Ohuchi, and Marjorie A. Olmstead, Appl. Phys. Lett. **87**, 171906 (2005).
[9] Taisuke Ohta, Andreas Klust, Jonathan A. Adams, Qiuming Yu, Marjorie A. Olmstead, and Fumio S. Ohuchi, Phys. Rev. B **69**, 125322 (2004).
[10] T. Ohta, D. A. Schmidt, S. Meng, A. Klust, A. Bostwick, Q. Yu, M. A. Olmstead, and F. S. Ohuchi, Phys. Rev. Lett. **94**, 116102 (2005).
[11] Fumio S. Ohuchi and Marjorie A. Olmstead, in *Encyclopedia of Electrical and Electronics Engineering*, edited by John G. Webster (Wiley, New York, 1999).
[12] A. Schneider and G. Gattow, Z. Anorg. Allg. Chem. **277**, 49 (1954).
[13] J. Ye, T. Yoshida, Y. Nakamura, and O. Nittono, Appl. Phys. Lett. **67**, 3066 (1995).
[14] J. Ye, S. Soeda, Y. Nakamura, and O. Nittono, Jpn. J. Appl. Phys., Part 1 **37**, 4264 (1998).
[15] D. Lübbers and B. Leute, J. Solid State Chem. **43**, 339 (1982).
[16] M. Peressi and A. Baldereschi, J. Appl. Phys. **83**, 3092 (1998).
[17] M. Ishikawa and T. Nakayama, Jpn. J. Appl. Phys., Part 1 **36**, L1576 (1997).
[18] T. Okamoto, N. Kojima, A. Yamada, M. Konagai, K. Takahasi, Y. Nakamura, and O. Nittono, Jpn. J. Appl. Phys., Part 2 **31**, L143 (1992).
[19] T. Nakayama and M. Ishikawa, J. Phys. Soc. Jpn. **66**, 3887 (1997).
[20] C.-S. Yoon, K-.H. Park, D.-T. Kim, T.-Y. Park, M.-S. Jin, S.-K. Oh, and W.-T. Kim, J. Phys. Chem. Solids **62**, 1131 (2001).
[21] Omicron Variable Temperature UHV Scanning Probe Microscope.
[22] J. A. Adams, Ph.D. thesis, University of Washington, 2004.
[23] V.-G. Kotlyar, A. A. Saranin, A. V. Zotov, T. V. Kasyanova, E. N. Chukurov, I. V. Pisarenko, and V. G. Lifshits, e-J. Surf. Sci. Nanotechnol. **3**, 55 (2005).